Rapid evolution of sexual size dimorphism facilitated by Y-linked genetic variance

Philipp Kaufmann[1*], Matthew E. Wolak[2], Arild Husby[1], Elina Immonen[1*]

[1]Evolutionary Biology, Department of Ecology and Genetics, Uppsala University, Norbyvägen 18D, 75234 Uppsala, Sweden.

[2]Department of Biological Sciences, Auburn University, Auburn, Alabama 36849, USA

Keywords: Sexual dimorphism, body size, experimental evolution, sexual conflict, animal model, Callosobruchus maculatus, sex chromosomes, Y chromosome, dominance variance

*Authors of correspondence: philipp.kaufmann@ebc.uu.se, elina.immonen@ebc.uu.se

Abstract

Sexual dimorphism is ubiquitous in nature, but its evolution is puzzling given that the mostly shared genome constrains independent evolution in the sexes. Sex differences should result from asymmetries between the sexes in selection or genetic variation, but studies investigating both simultaneously are lacking. Here, we combine a quantitative genetic analysis of body size variation, partitioned into autosomal and sex chromosome contributions, and 10-generations of experimental evolution to dissect the evolution of sexual body size dimorphism (SSD) in seed beetles (*Callosobruchus maculatus*) subjected to sexually antagonistic or sex-limited selection. Female additive genetic variance (V_A) was primarily linked to autosomes, exhibiting a strong intersexual genetic correlation with males ($r^a_{m,f}$ = 0.926), while X- and Y-linked genes further contributed to the male V_A, and X-linked genes contributed to female dominance variance. Consistent with these estimates, SSD did not evolve in response to female-limited selection, but evolved by 30-50% under male-limited and sexually antagonistic selection. Remarkably, Y-linked variance alone could change dimorphism by 30%, despite the *C. maculatus* Y chromosome being small and heterochromatic. Our results demonstrate how the potential for sexual dimorphism to evolve depends on both its underlying genetic basis and the nature of sex-specific selection.

Introduction

Sexual dimorphism is a defining feature of organisms with two sexes, manifested as a sex difference in the mean phenotypic values of traits in females and males [1–3]. The evolution of sexual dimorphism is favoured when there are sex differences in the fitness optima of a trait leading to differences in selection, including when a trait is under selection only in one sex, acts similarly on both sexes but differs in magnitude, or acts in opposite directions (i.e., is sexually antagonistic, SA). Such sex differences in selection are common in nature [4] owing to the different reproductive roles of females and males. How dimorphism evolves is also affected by the genetic architecture of trait variation. Most of the genome is shared between females and males, which is expected to constrain sexual dimorphism [5], but whether the constraint is absolute or quantitative should depend on sex specific genetic variance available to selection [6,7]. When alleles have sexually antagonistic fitness effects, selection on one sex can lead to the displacement of the other from its fitness optimum, a phenomenon known as intra-locus sexual conflict [8,9]. How this conflict is resolved lies at the heart of the evolution of sexual dimorphism. The degree to which shared alleles influence homologous traits in the sexes can be quantified with the intersexual genetic correlation, $r_{m,f}$ [5], which is typically high [10]. Sexual dimorphism has been difficult to alter with artificial sex-specific selection, suggesting its evolution can be strongly constrained by the $r_{m,f}$ and that sexual conflict may be persistent [11–14]. However, a high positive $r_{m,f}$ can deteriorate quickly when directly selected against[15] and it is not well understood if and how $r_{m,f}$ does constrain the evolution of SD.

One way to fully or partially escape a correlated response in both sexes is via linkage to sex chromosomes [16]. Intra-locus sexual conflict can be avoided by limiting the effects of sexually antagonistic alleles to the heterogametic sex by linkage to Y or W sex chromosomes [17]. However, Y and W chromosomes are typically dominated by large non-recombining regions subject to degenerative forces due to lower effective population size [18]. Old and highly heteromorphic sex chromosomes are thus gene poor with little capacity to maintain standing genetic variation for phenotypic traits [18]. Accordingly, there are few documentations of Y/W-linked variation in sexually dimorphic traits shared by the sexes in organisms with old sex chromosomes [19,20] (but see [21]). Effects of segregating Y-linked variation appear either very small for shared traits in the sexes [20,22] or are limited to male reproductive traits [23]. It is however increasingly recognized that Y linked genes can have more ubiquitous effects across tissues than previously believed [24],

challenging the view that Y linked genes are restricted to sex determination and primary reproductive functions [25]. This suggests that the Y chromosome may be underappreciated as a potential facilitator of sexual dimorphism [26].

Sexual conflict may also be partly resolved for X-linked sexually antagonistic alleles when male-beneficial alleles are recessive relative to female-beneficial alleles, thus increasing the fitness of female heterozygotes (the reverse applies to ZW systems) [16]. X or Z sex chromosomes have therefore been hypothesized to accumulate sexually antagonistic alleles [16], and by extension, facilitate the evolution of sexual dimorphism. Empirical support is however lacking and remains inconclusive [27–30]. Sexual conflict could also be partially resolved for the autosomal alleles via sex-specific dominance modifiers, whereby the favored allele in each sex is the more dominant one [30,31]. Empirical findings in salmonids [32,33] and beetles [34] support this possibility, but whether sex-specific dominance is common for sexually dimorphic traits is unknown.

Most empirical studies have thus far focused either on sex-specific selection [11–14] or on characterizing genetic variances in the sexes[10]. Yet, studying both simultaneously is necessary for assessing the degree to which $r_{m,f}$ limits the evolution of dimorphism and whether selection can overcome such constraints. Here we combine quantitative genetic pedigree analysis with replicated artificial selection to study how sexual body size dimorphism (SSD) evolves in *Callosobruchus maculatus* seed beetles when subjected to ten generations of sex-limited or sexually antagonistic selection. Our results demonstrate that a high intersexual genetic correlation need not constitute an absolute constraint, but that whether and how much SSD evolves depends critically on the nature of sex-specific selection and how it can act on sex-specific genetic variances.

Results

The sex-specific genetic architecture of body size

To characterise the quantitative genetic architecture of body size in each sex we analysed a four-generation double first cousin pedigree design with 8022 individuals (3981 females and 4041 males) using a Bayesian linear mixed effects model, allowing us to partition the phenotypic variance into additive and dominance genetic, maternal environment and residual variances. The total additive genetic variance (V_A) explains a

substantial part of the observed body size variance in both sexes, with a total narrow sense heritability ($h^2_{A,t}$) of 0.68 in females and 0.74 in males. We partitioned the total additive genetic variance (V_A) into autosomal (V_A^a), X- and Y-linked genetic variances (V_A^X and V_A^Y) (overview of the estimates in Fig. 1, details in Table 1 and Extended Data Fig. 1). While the overall additive genetic variance between the sexes is similar, the autosomal genetic variance is significantly higher in females than in males (see non-overlapping 95% CI: $V^a_{A,f}$ = 0.308, 95% CI (0.257, 0.356); $V^a_{A,m}$ = 0.147, 95% CI (0.116, 0.180)). Despite this difference, the autosomal intersexual genetic correlation is high ($r^a_{m,f}$= 0.924, 95%CI (0.846,0.994)), suggesting that the shared alleles have a similar phenotypic effect in the sexes. In females the majority of total additive genetic variance is accounted for by autosomal variance, as we detect no significant X-linked variance ($V^X_{A,f}$ = 0.010, 95% CI (0.000,0.033), $h^2_{X,f}$ = 0.022). We find a small amount of X-linked genetic variance in males. Although the lower 95% CI converged towards zero, there was a secondary peak in the distribution centred around the posterior mean (Extended Data Fig. 1f) that diverged substantially from the prior density providing support that the signal is not driven by the priors (this interpretation is also supported using likelihood ratio based model comparisons where X linked variance was significantly different from zero in males (Supplementary Table 4)). However, we cannot statistically infer that the $V^X_{A,f}$ is different from $V^X_{A,m}$ in either Bayesian (mean posterior distribution difference= -0.015, with 73% being smaller than -0.001) or likelihood based model (Supplementary Table 4).

Interestingly, we observe significant dominance variance (V_D) in females ($V_{D,f}$ = 0.067, 95 % CI (0.022,0.113), Extended Data Fig. 1g), but not in males ($V_{D,m}$ =0.021, 95% CI (0.000,0.054), Extended Data Fig. 1h). The difference between female and male dominance variance was 0.045 with approximately 93% of the posterior distribution of the difference greater than 0.001. Likelihood ratio based model comparison supports a significant sex difference in the dominance variance (Supplementary Table 4). Further partitioning the female dominance into variance attributed to the nine autosome pairs ($V^a_{D,f}$ = 0.022, 95% CI = (0.000, 0.063) and the single X-chromosomal pair ($V^X_{D,f}$ = 0.020, 95% CI = (0.000, 0.045)) suggests that a substantial part of the dominance variance is X-linked (Supplementary Table 1, Extended Data Fig. 2g&i), supported by a secondary peak in the posterior distribution for $V^X_{D,f}$. There is no significant maternal line variance in either sex, suggesting negligible variation in maternally transmitted cytoplasmic effects (e.g., mitochondrial).

Remarkably, Y-linked additive genetic variance has a similarly large effect on male body size as the total male autosomal additive genetic variance (V_A^Y = 0.154, 95% CI (0.117,0.191)). The Y lineages, potentially carrying different haplotypes, with a positive or negative Y-linked genetic effect (quantified from the posterior distributions for additive genetic effects of each potential Y lineage in our pedigree) increase or decrease average male body size, respectively, resulting in a significant correlation between the Y-lineage effect and male body size (adj. r^2 = 0.806, t = 16.61, p < 0.001, Extended Data Fig. 3). As expected, there is no such correlation between Y-lineage (patriline) effect and female body size (adj. r^2 = -0.002, t = 0.014, p = 0.989), although overall there is a significant correlation between male and female body size within patrilines (adj. r^2 = 0.103, t = 2.536, p = 0.0147). We further show that disregarding Y-linked genetic variance can lead to significantly biased estimates of sex-specific variances and dependent statistics, including the intersexual genetic correlation (Supplementary Table 2). Omitting Y-linked variance partitioning in our model significantly overestimates male autosomal additive genetic variance ($V_{A,m}^a$ = 0.287), heritability ($h_{a,m}^2$ = 0.713) and autosomal additive genetic variance for sexual dimorphism (V_{SSD}^a = 0.219), while underestimating the autosomal intersexual genetic correlation ($r_{m,f}^a$= 0.624).

In addition to characterising genetic variation in body size *per se*, we also found that there is additive autosomal genetic variance for sexual size dimorphism (V_{SSD}^a = 0.063, 95% CI (0.026,0.104)) (Table 1).

Size dimorphism evolves most rapidly under sexually antagonistic selection

We employed family-level artificial selection to test whether sexual size dimorphism evolves as a consequence of drift or in response to three different regimes of sex-limited selection (applied towards larger size in females and bi-directionally on males) or under sexually antagonistic selection to increase the naturally occurring SSD (towards larger females and smaller males). Each selection regime was replicated with two lines, and to propagate each line we selected 8 out of 56 families at each generation. The form of sexually antagonistic selection employed here is expected to directly target genetic variation in dimorphism [15] while sex-limited selection targets variation in body size *per se* but can do so differently in the sexes by acting on genetic variance specific to the sex under selection. During the 10 generations of selection, SSD evolved to become significantly different across generations and between selection regimes (χ_4^2 = 317.8, p < 0.001, more details provided in the Supplementary Table 3).

We first confirmed that drift did not alter the SSD in either replicate (empirical p-value; C_A = 0.813, C_B = 0.184, Fig. 2a), as neither sex changed in size (empirical p-values for male size; C_A = 0.393, C_B = 0.717; empirical p-values for female size; C_A = 0.461, C_B = 0.999). We next used these control lines to test how SSD evolved in each selection regime relative to the starting level, as using the control lines offered a replicated and balanced design for each comparison. Under sexually antagonistic selection we observed a significant and rapid increase in SSD by 49.7% (χ_1^2 = 117.8, p < 0.001, Fig. 2b). SSD evolved also under sex limited selection on males, with a significant increase by 31.7% (χ_1^2 = 28.48, p < 0.001, Fig. 2c) when selecting for small males and decrease by 27.8% (χ_1^2 = 25.59, p < 0.001, Fig. 2c) when selecting for large males. The observed changes in SSD under male limited selection are expected given the large Y-linked genetic variance and small X-linked variation observed in males that allow male-limited selection to change body size more in males than in females. In contrast, under female limited selection for large females we see no significant change in SSD (χ_1^2 = 0.038, p = 0.846, Fig. 2d), due to a strong correlated response to selection in males (male response: χ_1^2 = 229.9, p < 0.001, Fig. 3d), demonstrating how the high autosomal intersexual genetic correlation can constrain independent evolution in the sexes when selection cannot act on sex-specific additive variances (Table 1).

To further understand how each sex contributes to the evolution of sexual dimorphism, we tested for sex-specific changes in body size in each regime as compared to the drift control. While males evolved a significantly smaller size under sexually antagonistic selection (χ_1^2 = 28.0, p < 0.001), females did not significantly change (χ_1^2 = 0.580, p = 0.447) (Fig. 3b). The lack of female response is not due to lacking genetic variation as confirmed by both our quantitative genetic analysis (see above) and the observation that under female-limited selection female size increased rapidly and significantly (female response: χ_1^2 = 669.1, p < 0.0001), as did the male size (male response: χ_1^2 = 229.9, p < 0.001) (Fig. 3d). Male limited selection for small or large males also significantly changed body size in both sexes in the direction of selection (*small*: male response: χ_1^2 = 121.2, p < 0.001; female response: χ_1^2 = 96.34, p < 0.001; *large*: male response: χ_1^2 = 642.8, p < 0.001; female response: χ_1^2 = 261.5, p < 0.001) (Fig. 3c), although in both male limited selection experiments the change was more prominent in males resulting in a significant change in size dimorphism (see above).

Y chromosome is a major determinant of male size

To further examine the large Y-linked effect on variation in male body size, we introgressed the Y lineages remaining in the selection lines (and thus differently favoured by each selection regime) into a common isogenic background for 13 generations and then quantified the male and female body size in all 10 lines by measuring approximately 100 individuals of each sex. We found that a large difference in male size is retained between the lines, now genetically >99.97 % identical except for the introgressed Y chromosome (Fig. 4). Male body size is significantly different between the introgression lines (χ_4^2 = 137.4, p < 0.001). This is due to the males with a Y lineage favoured under selection for large size ($SL_m\uparrow$) retaining their significantly larger size compared to the males with Y lineages from any of the other selection lines, which amongst each other are no longer different (χ_3^2 = 2.894, p = 0.408). In contrast, when we compare female body size in the $SL_f\uparrow$ and $SL_m\downarrow$ introgression lines, the regimes that had the largest and smallest females after selection, respectively, we see no significant difference (χ_1^2 = 2.480, p = 0.1153). Consequently, sex difference in body size is significantly reduced, by 30%, in the introgression lines with a large male Y haplotype relative to those with a small male haplotype (χ_4^2 = 145.0, p < 0.001, Fig. 4), demonstrating that the Y chromosome alone can drastically alter the sexual size dimorphism.

Discussion

We have characterised the sex-specific genetic architecture underlying body size and tested how sexual size dimorphism responds to ten generations of sexually antagonistic or sex-limited selection. In contrast to previous work [12,14], we find that size dimorphism evolves rapidly under sexually antagonistic selection and in response to both upward and downward selection limited to males. Interestingly, however, size dimorphism did not evolve in response to selection operating only on females. These results demonstrate how the nature of sex-specific selection is a critical determinant of how sexual dimorphism evolves. Our results are compatible with linkage to the X chromosome and sex-specific dominance, two core mechanisms proposed to facilitate the evolution of sexual dimorphism [16,31,35] but which has so far received limited empirical support [29,31,36]. Further, we show that the Y chromosome plays a major role in facilitating sex-

196 specific evolution of body size, demonstrating that Y linkage can resolve the sexual conflict over a polygenic
197 trait shared by the sexes, despite being small in size and highly heterochromatic [37,38].
198 The strong effect of Y-linked additive genetic variance, explaining over 30% of the observed male
199 body size variation, offers an immediate resolution to sexual conflict over body size by being male limited [17],
200 but is also unusual and unexpected. In *C. maculatus*, as in many XY systems, the sex chromosomes are
201 highly diverged [37,38] and in line with absence of recombination, the Y sequences are rich in repeats and poor
202 in genes [37]. It is therefore challenging to understand how functional genetic variation has been maintained on
203 the Y in the face of drift. A possible answer to this may lie in frequency dependent selection that has the
204 potential to maintain Y polymorphism [39–41].
205 Although unlikely to explain the maintenance of Y-linked polymorphism, it is possible that some of
206 the Y-linked variance detected is also attributable to genetic variance in other genomic regions involved in
207 epistatic interactions with the Y-linked loci [23,42] that may together affect male body size variation. In
208 *Drosophila* Y-linked loci can be trans-acting regulatory factors for thousands of autosomal genes involved in
209 not only reproduction but also metabolism [43], and epistatic interactions between the sex chromosomes and
210 autosomes can even be expected due their antagonistic coevolution [44]. In our population the female
211 autosomal additive variance is as high as male autosomal and Y-linked additive genetic variances together,
212 which may indicate that the effect of autosomal genetic variance in males depends on the Y lineage. This is
213 further supported by our introgression of the different Y-lineages from the selection lines to an isogenic
214 background, which demonstrates that in the absence of other genetic variation, there are only two
215 distinguishable male size variants responsible for changing dimorphism. Yet, the Y-linked effect uncovered
216 in the pedigree analysis reveals more continuous Y-linked effects on body size variation in males (Extended
217 Data Fig. 3a). Together, these results suggest epistatic interactions between the genetic variation in the Y
218 and autosomes or the X chromosome.
219 While the Y chromosome is a prime candidate to facilitate sexual dimorphism it is often neglected
220 under the assumption of a lack of genes or segregating non-neutral polymorphisms [18]. While Y-linked
221 genetic variance is indeed often limited in degenerated heteromorphic chromosomes (reviewed in [45]) our
222 results demonstrate that they should nevertheless be investigated in a quantitative genetics framework. Using
223 empirical data we could show that not accounting for Y-linked genetic variance can significantly bias other
224 variance estimates in the model and subsequently the autosomal intersexual genetic correlation

(Supplementary Table 2), an argument that has been made for sex-linked genetic variance in general [28], although not with focus on genetic variance on the Y (or W) chromosome.

In line with the finding of male limited genetic variance for body size, SSD could evolve under selection regimes where selection targets males (i.e., under SA and male limited selection). In contrast, it did not change under female limited selection (or due to drift), demonstrating how the high $r^a_{m,f}$ due to shared autosomal genetic variation causes a correlated evolutionary response in males. Selection in males targets Y-linked variation in an expected way (Extended Data Fig. 4): Y lineages associated with small male body size are prevalent in SA and small-male selection lines, while Y lineages associated with large male body size were favoured under selection for large males. However, the evolution of sexual dimorphism cannot be explained by Y-linked genetic variance alone. Given that the Y chromosome is expected to act like a single major effect locus, it should become rapidly fixed under strong selection, which is also what we see in our experiments (Extended Data Fig. 4a). But in the lines where SSD increased (i.e., $SL_m\downarrow$ and SA), sex difference continued to increase linearly throughout the selection experiment even after Y linked variation was eroded, strongly suggesting that additional genetic variation has facilitated SSD. The family-level selection applied here allows for selection to also target nonadditive genetic variance such as dominance variance detected in females (Table 1, Supplementary Table 3). Together with small amounts of X-linked additive variance in males as well as autosomal additive genetic variance for dimorphism captured by V^a_{SSD} these genetic variances likely contribute to this continued evolution of size dimorphism (Fig. 2, Extended Data Fig. 4a), but may do so differently depending on the selection applied. While SSD increased in both, only SA selection prevented a correlated response in female size resulting in a greater change (i.e., up to 50% under SA selection in contrast to <30% in $SL_m\downarrow$). Female-specific dominance may have played a role here to maintain female size at the ancestral level, given that this is the only detected female-specific variance component. Unlike sex-limited directional selection, SA selection has the potential to maintain the genetic variance [46] necessary for dominance effects to manifest themselves as dominance variance [31]. Further partitioning of female dominance variance into X-linked and autosomal dominance suggests that, despite the size difference of these two genetic regions, both X-linked and autosomal dominance variance contribute equally to the overall female dominance variance (Supplementary Table 1 and Extended Data Fig. 2g&i). While sex-specific dominance both on the autosomes and the X is evoked by theory to partially resolve the

intralocus sexual conflict[16,30,31], it is still unclear whether it may actually contribute to the evolution of sexual dimorphisms. Our results indicate that this could indeed be the case.

Conclusions

Previous experimental and theoretical work has shown that sexually antagonistic selection is relatively inefficient in terms of changing sexual dimorphism, due to a high intersexual genetic correlation [14,47]. Here, we show that even when the sexes share most of the autosomal genetic variation, dimorphism can readily evolve when selection can target sex-specific genetic variances. The strikingly large Y-linked genetic variance in our beetle population is an interesting demonstration that even a degenerated Y chromosome can contribute substantially to the evolution of sexual dimorphism. Y chromosomes can clearly have a broader role in males beyond determining primary reproductive traits and facilitate sexual dimorphism also in sexually homologous traits, a role that may often remain enigmatic due to a lack of segregating Y-linked genetic variance. The Y-linkage together with the sex-specific dominance variance, X-linked variance and autosomal genetic variance for SSD, suggest that multiple mechanisms could contribute to resolving sexual conflict in polygenic traits.

Methods

Study organism

The seed beetle *Callosobruchus maculatus* is a common pest of legume seeds in subtropical and tropical regions. Females oviposit directly onto seeds that serve as food source and environment for the larval development, which lasts approx. 25 days (at 29 °C, 50% RH and a 12:12 light:dark cycle [48]). Adult *C. maculatus* is an aphagous capital breeder with an ability to finish its entire reproductive cycle using the larval resources. Across all our experiments body mass acquisition thus happens exclusively during the larval stages within the seed. In adult beetles fecundity selection favors larger female size and sexual competition smaller male size, subjecting body size to sexually antagonistic selection [34,49,50]. *C. maculatus* has 18 autosomes in addition to XY sex chromosomes.

The *C. maculatus* study population was founded by beetles isolated from a set of *Vigna unguiculata* seeds that were collected at a single agricultural field close to Lome, Togo in 2010. Initially, 41 isofemale lines were established by randomly pairing virgin males and females that emerged from these seed pods. A panmictic population was subsequently formed by pooling all 41 isofemale lines and was kept on *Vigna radiata* beans under benign conditions for 10 generations prior to the experiment. Once the majority of adults emerged (day 27), they were transferred to a new set of beans for oviposition for 10 days, before they were removed to ensure non-overlapping generations.

Quantifying genetic variation in body size

The pedigree design

To characterize the quantitative genetic architecture of body size and size dimorphism in *C. maculatus* we adapted a breeding design proposed by Fairbairn & Roff [51] to specifically partition sex-linked and dominance genetic variances, in addition to autosomal additive genetic variances and their cross-sex covariance. The breeding design builds upon the comparison of (single & double) first cousins and (half & full) siblings and therefore consists of at least three generations. The version we used in this study had 4 generations, referred to as Grandparents (GP), Parents (P), Offspring1 (F1) and Offspring2 (F2) (Additional Supplementary Fig. 1).

We measured body size as weight [mg] of all GP, P, F1 and F2 adults individually within 24h after emergence. To ensure body size measurement within 24h and thus minimize potential aging effects, individuals were measured in parallel by two researchers. All crosses were performed by pairing an adult female and adult male in a 1.5ml Eppendorf for one hour. Afterwards, only the female was transferred to a Petri dish with 18g *V. radiata* beans, to oviposit for 24 hours.

To achieve consistent conditions throughout the four generations of interest, and to limit any cross-generational parental effects, we created a controlled environment two generations in advance. Adult *C. maculatus* collected from the meta population - the great-great-grandparents (GGGP) - were allowed to lay eggs for a limited time window of 48h, which controls for density and unifies the age of the next generation. GGP adults were collected as virgins by isolating the host beans prior to their emergence (5 days prior to the expected emergence date). In this study, we used only beans that carried one egg and therefore

only one growing larva inside, to rule out any potential resource competition in the bean and to facilitate the collection of virgins. To establish the next generation, the adult GGP females and males were paired randomly (avoiding full-sibling crosses). We prepared 240 GGP crossings to give rise to 240 GP families.

GP generation: GP individuals were collected as virgins, sexed and body mass measured. We then randomly crossed the GP to generate five P families in each breeding set replicate (Additional Supplementary Fig. 1) in the same way as described above.

P generation: For each of the 5 P families in a breeding set, we randomly selected four adults, two males and two females, for family P_1 and P_2 and 4 females for families P_3, P_4 and P_5. Each male was mated sequentially to four unrelated virgin females to form half-sib families, with one female from each of the four P families. To do this, each male was paired with a female in an Eppendorf tube for 1h, then transferred into an empty Eppendorf tube to rest for an hour and paired up with the next female for another hour. Once the male was mated with all four females, we discarded the male and transferred the mated females individually into Petri dishes for 24h of oviposition. We randomized the order of the crossings, but also recorded the mating order to correct for any such putative effect in our analyses.

F1 offspring: From each F1 family we randomly selected one male and female for the subsequent breeding of the F2 generation. Selected virgin F1 individuals were crossed randomly (avoiding full-sibling crosses) across all 24 breeding set replicates.

F2 offspring: Similar to the F1 generation, we randomly selected one male and female for each F2 family to generate the initial generation (G0) for the consecutive artificial selection experiment (see more details below).

Overall, the pedigree for the quantitative genetics experiment contains 8022 beetles (3981 females and 4041 males) that were reared and measured under standardized, controlled laboratory conditions.

Quantitative genetic pedigree analyses:

The pedigree analysis was performed with a mixed effect model, known as the animal model. All data was analysed using the software R, version 3.4.0 [52].

To characterize the genetic architecture of body size and ultimately sexual size dimorphism in *C. maculatus* we constructed a GLMM with Gaussian errors and an identity link function using the R package MCMCglmm [53] that allows us to estimate sex-specific genetic variances, covariances and associated

statistics of interest in a Bayesian framework. We modelled body size as a bivariate trait that is normally distributed in both sexes (Extended Data Fig. 5). We estimated sex-specific, autosomal additive genetic variance (V_A^a) and the cross-sex autosomal additive covariance ($COV\left(A_f^a, A_m^a\right)$), sex-specific X-linked additive genetic variance (V_A^X) and sex-specific autosomal dominance variance (V_D^a). Dominance and X-linkage covariances were fixed to zero *a priori*. Additionally, we estimated male specific Y-linked additive variance (V_A^Y) by fitting random effects of the founding male ancestor individuals and maternal environment effects (V_{ME}**)**. We used parameter expanded priors, but also explored the robustness of our results by using more informative priors (results not shown). In our model we corrected for the two different researchers performing the phenotyping, P crossing order, and effects of the developmental time on body size in each sex by fitting them as fixed effects. The additive, dominance and X-linked (co)-variance relationship matrices were calculated using the NADIV R package [54].

Additionally, we also used a likelihood based animal model to verify our results (Extended Data Fig. 1) and to conduct model comparisons using the software ASReml-R 4.0 (described in Supplementary Table 4).

Calculations of associated statistics included autosomal sex-specific narrow sense heritability for males and females:

$$V_{z,m} = V_{A,m}^a + V_{A,m}^X + V_{A,m}^Y + V_{D,m}^a + V_{ME,m} + V_{r,m}$$

$$V_{z,f} = V_{A,f}^a + V_{A,f}^X + V_{D,f}^a + V_{ME,f} + V_{r,f}$$

$$h_{a,m}^2 = \frac{V_{A,m}^a}{V_{z,m}}$$

$$h_{a,f}^2 = \frac{V_{A,f}^a}{V_{z,f}}$$

Where $V_{r,m}$ and $V_{r,f}$ represent the residual variance for males and females, respectively.

Intersexual autosomal additive genetic correlation was calculated as:

$$r_{m,f}^a = \frac{COV\left(A_f^a, A_m^a\right)}{\sqrt{V_{A,m}^a \times V_{A,f}^a}}$$

Sex-specific, X- and Y-linked narrow sense heritability;

$$h_{X,m}^2 = \frac{V_{A,m}^X}{V_{z,m}}$$

$$h^2_{X,f} = \frac{V^X_{A,f}}{V_{z,f}}$$

$$h^2_{Y,m} = \frac{V^Y_{A,m}}{V_{z,m}}$$

And total sex-specific narrow sense heritability as:

$$h^2_{t,A,m} = h^2_{a,m} + h^2_{X,m} + h^2_{Y,m}$$

$$h^2_{t,A,f} = h^2_{a,f} + h^2_{X,f}$$

Additionally we calculated the autosomal additive genetic variance of the sexual size dimorphism (SSD) according [55] as:

$$V^a_{SSD} = V^a_{A,m} + V^a_{A,f} - 2COV\left(A^a_f, A^a_m\right)$$

Artificial selection on body size

Our second aim in this study was to test whether and how sexual dimorphism can evolve under different sex-specific selection regimes, using artificial family-level selection. We quantified sexual dimorphism as a ratio of female to male body size within a family. We used family level selection as a tool to screen for genetic variation contributing to divergent phenotypic expression in the sexes, i.e., to select on the variation in sexual dimorphism, for which brother-sister dimorphism serves as a proxy because such variation is otherwise hard to quantify. Additionally, family level selection allows for a strict control of drift among the different selection and control lines.

The starting generation (G0) for all selection lines was directly established by using the offspring from the F2 generation of the quantitative genetic pedigree experiment. For this, 311 male and 311 female F2 individuals were paired randomly, while avoiding full-sib mating, in a 1.5ml Eppendorf for one hour, followed by 24h of oviposition on *V. radiata*. For each F2 mating pair we isolated 24 beans to collect male and female virgins from the same family. We measured the average female and male body mass [mg] for each family, by pooling 7 individuals of each respective sex. Throughout the artificial selection experiment we kept track of the pedigree on a family-level, which allows us to trace both the maternal and paternal line back to the GGP generation in the quantitative genetic pedigree experiment.

We created two types of selection scenarios – sexually antagonistic (SA) selection and sex-limited (SL) selection – the latter of which applied in three different ways, as well as a drift control, resulting in a total of 5 selection regimes. In the SA regime we selected for families with the largest relative sexual size dimorphism (i.e., largest ratio of the female to male average body size). The SL regimes, where we only selected on the body size of one sex, include bidirectional selection on males ($SL_m\downarrow$: selection for families with smallest males, $SL_m\uparrow$: selection for families with largest males), and selection for large females ($SL_f\uparrow$: families with largest females. Unidirectional due to logistic reasons). In the control regime we selected families randomly, as a control for genetic drift. Each regime was replicated twice, resulting in a total of 10 lines.

To start each selection line, we selected 8 families from the same founder generation (G0). Because each selection line was started from the same base population, there was some overlap between the replicates and also selection regimes in the initial selection step. I.e., a family that would have been selected for its large females ($SL_f\uparrow$) could also have been selected for its large males ($SL_m\uparrow$). To avoid any bias, we distributed the families in a balanced way, by following a list of priority for each line, and assigned families in an alternating way until the required number was reached. Once eight families were assigned to each selection line we crossed them to produce the next generation. Families were crossed in a fully factorial way, but avoiding any full sib crossings, resulting in 56 families to form the next generation for each selection line. Mating pairs were crossed directly in a Petri dish prepared with *V. radiata*, where they could mate and oviposit for 48h, after which both adults were removed. At each subsequent generation of selection, 24 beans for each family (56 families x 10 lines) were isolated 5 days prior to their expected adult emergence date. We continued the selection for 10 generations, by always selecting 8 out of the 56 families in each selection line, based on the selection criteria of the respective selection regime. Crossings that failed to produce 7 females and 7 males could not be used for the factorial crossings and were therefore not considered in the selection.

Statistical analyses of the selection lines

To infer whether the artificial selection changed the relative sexual size dimorphism we used a linear mixed effect model that included all 5 selection regimes using the lme4 R package. Here, we fitted generation and the selection regime as fixed effects, with the line replicate (n=10) as a random factor (nested within selection regime).

To address whether drift alone can change SSD over the course of the artificial selection lines, we contrasted SSD in each drift control replicate at generation 10 (n = 8 families) to the founding population at generation 0 (n = 161 families). To account for the unbalanced sample size, we used random resampling and calculated an empirical p-value for each replicate line (C_A and C_B). We then performed pairwise comparisons of each selection regime to the drift control, using the mixed effect model outlined above. We performed the same analysis for male and female body size as a response variable, respectively.

Y chromosome introgression

Both results from the quantitative genetic pedigree analysis and the artificial selection experiment pointed to a strong effect of Y-linkage. To isolate the effect of the Y chromosome from genetic variation in the rest of the genome, we introgressed the different Y-lineages uncovered from the selection experiment into an isogenic background (generated by >20 generations of inbreeding [34]) by repeatedly backcrossing males to the isogenic females for 13 generations. In particular, for each selection line and replicate we used 3 randomly chosen virgin males and crossed them each with one virgin female from the inbred population in a 60mm Petri dish with 18g *V. radiata* beans. For the selection lines that had more than 1 potential Y-lineage present after 10 generations of artificial selection (i.e., C_A, C_B and SA_B), we randomly chose one of the Y-lineages for introgression. In the consecutive generations we again used 3 virgin males (1 randomly chosen son from each father) to backcross them with inbred virgin females. Over the course of this process, we introgressed the different Y-lineages into a genetically isogenic common garden. This set up allowed us to therefore isolate the effect of the Y chromosome haplotype on body size. To quantify the phenotypic effect of the Y-lineages on male body size in a genetically isogenic common garden after 13 generations (i.e., >99.97% genetic similarity, except for the Y chromosome), we created a controlled environment for 2 generations in advance to the phenotyping. For each Y-introgression line we used 3 males that were paired in a Petri dish with an isogenic female each, forming 3 Petri dish groups in each line. We also set up density controlled crosses of the isogenic background, to minimize potential density and age related effects from the maternal side. For each Petri dish group we then isolated 3 virgin males and mated them to a density controlled isogenic female each, to generate offspring that we phenotyped in the next generation. We individually measured ~100 females and ~100 males for each Y-introgression line, using the same protocol as described in the quantitative genetic pedigree experiment.

Statistical analysis of the Y-introgression lines

To test whether the SSD changes based on the introgressed Y-lineage, we first calculated the relative SSD by dividing the average female and male size within each Petri dish group. We then used a mixed effect model with selection regime as a fixed effect and replication as a nested random effect, to test for differences among lines. The model was fitted separately for the sexes.

Data availability

Data generated and analysed in this study are available in the Dryad repository [56] (https://doi.org/10.5061/dryad.dfn2z350x).

Code availability

R code for the MCMCglmm and ASReml-R 4.0 is provided in the supplementary information.

Acknowledgements

The authors thank J. Liljestrand-Rönn for help in the laboratory and D. Scofield for computational support. We also thank the beetle research group at Uppsala University for valuable discussions, G. Arnqvist and S. Karrenberg for comments on the earlier draft of the manuscript, and three reviewers for their valuable critique and suggestions that further improved this manuscript. The computations were enabled by resources in project SNIC 2019/8-55 provided by the Swedish National Infrastructure for Computing at UPPMAX, partially founded by the Swedish Research Council. This work was funded by the grants from the Swedish Research Council (grant no. 2019-05038) and Carl Trygger Foundation (grant no. CTS-18:163) to E.I.

Competing interests

The authors declare no competing interests.

Author contribution statement

The study idea and the general experimental design were conceived by E.I., while P.K. developed further the details of the experimental design, carried out the experiments and collected the data with assistance from E.I. Data analysis and preparation of results was done by P.K. with input and assistance from E.I, M.E.W

and A.H. The initial manuscript was written by P.K and E.I. with substantial contributions from all the authors on later versions of the manuscript.

References:

1. Darwin, C. *The Descent of Man, and Selection in Relation of Sex*. (1871).
2. Andersson, M. *Sexual Seleciton*. (Princeton University Press, 1994).
3. Fairbairn, D. J. *Odd Couples: Extraordinary Differences between the Sexes in the Animal Kingdom*. (Princeton University Press, 2013).
4. Cox, R. M. & Calsbeek, R. Sexually antagonistic selection , sexual dimorphism , and the resolution of intralocus sexual conflict. *Am. Nat.* **173,** 176–187 (2009).
5. Lande, R. Sexual dimorphism, sexual selection, and adaptation in polygenic characters. *Evolution* **34,** 292–305 (1980).
6. Mezey, J. G. & Houle, D. The dimensionality of genetic variation for wing shape in Drosophila melanogaster. *Evolution* **59,** 1027–1038 (2005).
7. Gomulkiewicz, R. & Houle, D. Demographic and genetic constraints on evolution. *Am. Nat.* **174,** 218-229 (2009).
8. Rice, W. R. & Chippindale, A. K. Intersexual ontogenetic conflict. *J. Evol. Biol.* **14,** 685–693 (2001).
9. Bonduriansky, R. & Chenoweth, S. F. Intralocus sexual conflict. *Trends Ecol. Evol.* **24,** 280–288 (2009).
10. Poissant, J., Wilson, A. J. & Coltman, D. W. Sex-specific genetic variance and the evolution of sexual dimorphism: A systematic review of cross-sex genetic correlations. *Evolution* **64,** 97–107 (2010).
11. Delph, L. F., Gehring, J. L., Frey, F. M., Arntz, A. M. & Levri, M. Genetic constraints on floral evolution in a sexually dimorphic plant revealed by artificial selection. *Evolution* **58,** 1936–1946 (2004).
12. Tigreros, N. & Lewis, S. M. Direct and correlated responses to artificial selection on sexual size dimorphism in the flour beetle, Tribolium castaneum. *J. Evol. Biol.* **24,** 835–842 (2011).
13. Reeve, J. P. & Fairbairn, D. J. Sexual size dimorphism as a correlated response to selection on body size: An empirical test of the quantitative genetic model. *Evolution* **50,** 1927–1938 (1996).
14. Stewart, A. D. & Rice, W. R. Arrest of sex-specific adaptation during the evolution of sexual dimorphism in Drosophila. *Nat. Ecol. Evol.* **2,** 1507–1513 (2018).

15. Delph, L. F., Steven, J. C., Anderson, I. A., Herlihy, C. R. & Brodie, E. D. Elimination of a genetic correlation between the sexes via artificial correlational selection. *Evolution* **65,** 2872–2880 (2011).
16. Rice, W. R. Sex chromosomes and the evolution of sexual dimoprhism. *Evolution* **38,** 735–742 (1984).
17. Rice, W. R. Evolution of the Y sex chromosome in animals. *Bioscience* **46,** 331–343 (1996).
18. Charlesworth, B. & Charlesworth, D. The degeneration of Y chromosomes. *Philos. Trans. R. Soc. Lond. B. Biol. Sci.* **355,** 1563–1572 (2000).
19. Delph, L. F., Arntz, A. M., Scotti-Saintagne, C. & Scotti, I. The genomic architecture of sexual dimorphism in the dioecious plant Silene latifolia. *Evolution* **64,** 2873–2886 (2010).
20. Griffin, R. M., Le Gall, D., Schielzeth, H. & Friberg, U. Within-population Y-linked genetic variation for lifespan in Drosophila melanogaster. *J. Evol. Biol.* **28,** 1940–1947 (2015).
21. Charlesworth, D. The guppy sex chromosome system and the sexually antagonistic polymorphism hypothesis for y chromosome recombination suppression. *Genes* **9,** (2018).
22. Evans, S. R., Schielzeth, H., Forstmeier, W., Sheldon, B. C. & Husby, A. Nonautosomal genetic variation in carotenoid coloration. *Am. Nat.* **184,** 374–383 (2014).
23. Chippindale, A. K. & Rice, W. R. Y chromosome polymorphism is a strong determinant of male fitness in Drosophila melanogaster. *Proc. Natl. Acad. Sci. U. S. A.* **98,** 5677–5682 (2001).
24. Skaletsky, H. *et al.* The male-specific region of the human Y chromosome is a mosaic of discrete sequence classes. *Nature* **423,** 825–837 (2003).
25. Maan, A. A. *et al.* The y chromosome: A blueprint for men's health? *Eur. J. Hum. Genet.* **25,** 1181–1188 (2017).
26. Prokop, J. W. & Deschepper, C. F. Chromosome Y genetic variants: Impact in animal models and on human disease. *Physiol. Genomics* **47,** 525–537 (2015).
27. Ruzicka, F. & Connallon, T. Is the X chromosome a hot spot for sexually antagonistic polymorphisms? Biases in current empirical tests of classical theory. *Proc. R. Soc. Lond. B*. **287,** (2020).
28. Husby, A., Schielzeth, H., Forstmeier, W., Gustafsson, L. & Qvarnström, A. Sex chromosome linked genetic variance and the evolution of sexual dimorphism of quantitative traits. *Evolution* **67,** 609–619 (2013).

29. Dean, R. & Mank, J. E. The role of sex chromosomes in sexual dimorphism: Discordance between molecular and phenotypic data. *J. Evol. Biol.* **27,** 1443–1453 (2014).

30. Fry, J. D. The genomic location of sexually antagonistic variation: Some cautionary comments. *Evolution* **64,** 1510–1516 (2010).

31. Spencer, H. G. & Priest, N. K. The evolution of sex-specific dominance in response to sexually antagonistic selection. *Am. Nat.* **187,** 658–666 (2016).

32. Barson, N. J. *et al.* Sex-dependent dominance at a single locus maintains variation in age at maturity in salmon. *Nature* **528,** 405–408 (2015).

33. Pearse, D. E. *et al.* Sex-dependent dominance maintains migration supergene in rainbow trout. *Nat. Ecol. Evol.* **3,** 1731–1742 (2019).

34. Grieshop, K. & Arnqvist, G. Sex-specific dominance reversal of genetic variation for fitness. *PLoS Biol.* **16,** 1–21 (2018).

35. Reinhold, K. & Engqvist, L. The variability is in the sex chromosomes. *Evolution* **67,** 3662–3668 (2013).

36. Mank, J. E. & Ellegren, H. Sex-linkage of sexually antagonistic genes is predicted by female, but not male, effects in birds. *Evolution* **63,** 1464–1472 (2009).

37. Sayadi, A. *et al.* The genomic footprint of sexual conflict. *Nat. Ecol. Evol.* **3,** 1725–1730 (2019).

38. Angus, R. B., Dellow, J., Winder, C. & Credland, P. F. Karyotype differences among four species of Callosobruchus Pic (Coleoptera: Bruchidae). *J. Stored Prod. Res.* **47,** 76–81 (2011).

39. Van Hooft, P. *et al.* Rainfall-driven sex-ratio genes in African buffalo suggested by correlations between Y-chromosomal haplotype frequencies and foetal sex ratio. *BMC Evol. Biol.* **10,** (2010).

40. Postma, E., Spyrou, N., Rollins, L. A. & Brooks, R. C. Sex-dependent selection differentially shapes genetic variation on and off the guppy Y chromosome. *Evolution* **65,** 2145–2156 (2011).

41. Clark, A. G. Natural selection and Y-linked polymorphism. *Genetics* **115,** 569–577 (1987).

42. Jiang, P. P., Hartl, D. L. & Lemos, B. Y not a dead end: Epistatic interactions between Y-linked regulatory polymorphisms and genetic background affect global gene expression in Drosophila melanogaster. *Genetics* **186,** 109–118 (2010).

43. Lemos, B., Araripe, L. O. & Hartl, D. L. Polymorphic Y chromosomes harbor cryptic variation with manifold functional consequences. *Science* **319,** 91–93 (2008).

44. Lund-Hansen, K. K., Olito, C., Morrow, E. H. & Abbott, J. K. Sexually antagonistic coevolution between the sex chromosomes of Drosophila melanogaster. *Proc. Natl. Acad. Sci. U. S. A.* **118,** (2021).

45. Sayres, M. A. W. Genetic Diversity on the Sex Chromosomes. *Genome Biol. Evol.* **10,** 1064–1078 (2018).

46. Connallon, T. & Clark, A. G. Balancing selection in species with separate sexes: Insights from fisher's geometric model. *Genetics* **197,** 991–1006 (2014).

47. McGlothlin, J. W., Cox, R. M. & Brodie, E. D. Sex-specific selection and the evolution of between-sex genetic covariance. *J. Hered.* **110,** 422–432 (2019).

48. Arnqvist, G. & Tuda, M. Sexual conflict and the gender load: Correlated evolution between population fitness and sexual dimorphism in seed beetles. *Proc. R. Soc. B Biol. Sci.* **277,** 1345–1352 (2010).

49. Berger, D., Berg, E. C., Widegren, W., Arnqvist, G. & Maklakov, A. A. Multivariate intralocus sexual conflict in seed beetles. *Evolution* **68,** 3457–3469 (2014).

50. Berger, D. *et al.* Intralocus sexual conflict and the tragedy of the commons in seed beetles. *Am. Nat.* **188,** 98–112 (2016).

51. Fairbairn, D. J. & Roff, D. A. The quantitative genetics of sexual dimorphism: Assessing the importance of sex-linkage. *Heredity* **97,** 319–328 (2006).

52. R Core Team. R: A language and environment for statistical computing. (2020).

53. Hadfield, J. D. MCMC methods for multi-response generalized linear mixed models: The MCMCglmm R package. *J. Stat. Softw.* **33,** 1–22 (2010).

54. Wolak, M. E. Nadiv: An R package to create relatedness matrices for estimating non-additive genetic variances in animal models. *Methods Ecol. Evol.* **3,** 792–796 (2012).

55. Lynch, M. & Walsh, B. *Genetics and Analysis of Quantitative traits*. (Sinauer Assocs., 1998).

56. Kaufmann, P. & Immonen, E. Rapid evolution of sexual size dimorphism facilitated by Y-linked genetic variance DATA SET. Dryad repository. doi:https://doi.org/10.5061/dryad.dfn2z350x. (2021)

Tables:

Table 1| Results from the quantitative genetic analysis. Posterior genetic variance estimates mean, [posterior mode] and (95% credible interval). Values in bold are significantly different from zero. Estimates that changed significantly when not accounting for V_A^Y partitioning (i.e. are outside of the 95% credible interval of a less complex model) are highlighted with ‡ or ⭳ if they would get significantly over- or underestimated in the simpler model, respectively (see simpler model in Supplementary Table 1). The model was run on 16 independent Markov chains in parallel for 670,000 iterations (burn in 20,000, thinning interval 650) yielding 1,000 samples for each chain and 16,000 samples across all chains. Absolute autocorrelation values are < 0.125 and the effective sample size > 11,500 for each posterior distribution.

	Additive (co)variance					**Dominance variance**	**Maternal environment**	**Residual Variance**
	autosomal		X-linked	Y-linked	total			
Female body size	$V^a_{A,f}$ **= 0.308** [0.305] (0.257,0.356)	COV^a_A **= 0.196** [0.197] (0.169,0.223)	$V^X_{A,f}$ = 0.010 [0.000] (0.000,0.033)		$V_{A,f}$ **= 0.318** [0.325] (0.273,0.364)	$V_{D,f}$ **= 0.067** [0.066] (0.022,0.113)	$V_{ME,f}$ = 0.004 [0.000] (0.000,0.013)	$V_{R,f}$ **= 0.076** [0.069] (0.033,0.118)
Male body size	$V^a_{A,m}$ **= 0.147** ‡ [0.151] (0.116,0.180)	$r^a_{m,f}$**= 0.924** ⭳ [0.944] (0.846,0.994)	$V^X_{A,m}$ = 0.025 [0.000] (0.000,0.056)	V^Y_A **= 0.154** [0.151] (0.117,0.191)	$V_{A,m}$ **= 0.325** [0.317] (0.273,0.379)	$V_{D,m}$ = 0.021 [0.000] (0.000,0.054)	$V_{ME,m}$ = 0.002 [0.000] (0.000,0.006)	$V_{R,m}$ **= 0.090** ⭳ [0.096] (0.061,0.118)
Sexual dimorphism	V^a_{SSD}**= 0.063** ‡ [0.058] (0.026,0.104)							
Female heritability	$h^2_{a,,f}$ **= 0.662** [0.683] (0.575,0.742)		$h^2_{X,f}$ = 0.022 [0.000] (0.000,0.070)		$h^2_{t,A,f}$ **= 0.684** [0.683] (0.615,0.753)			
Male heritability	$h^2_{a,,m}$ **= 0.335** ‡ [0.337] (0.258,0.409)		$h^2_{X,m}$ = 0.056 [0.001] (0.000,0.124)	$h^2_{Y,m}$ **= 0.350** ⭳ [0.344] (0.292,0.409)	$h^2_{t,A,m}$ **= 0.741** [0.745] (0.675,0.801)			

Figures:

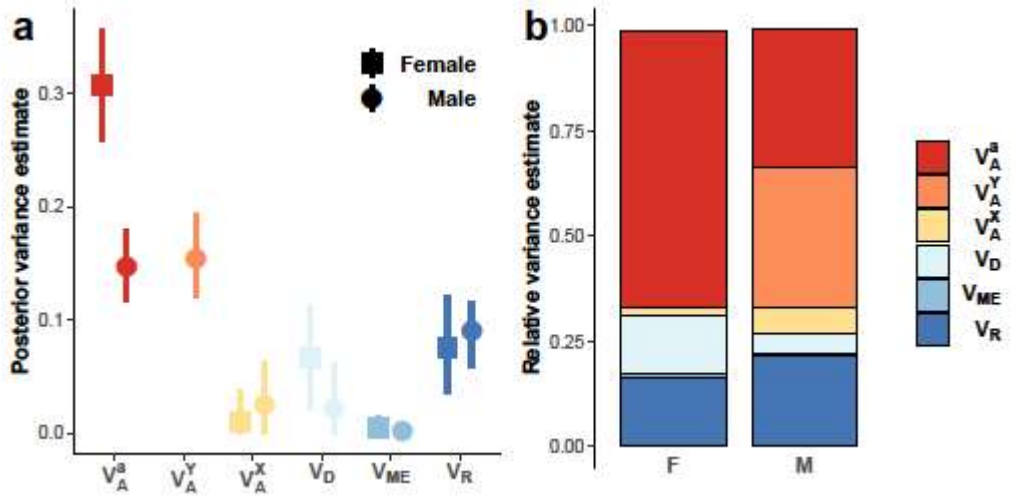

Fig. 1| Overview of the posterior estimates for genetic variances. a) Mean genetic variance estimates (square & circle) and their 95% credible interval (vertical line). **b)** Proportion of phenotypic body size variance explained by genetic variances in each sex (i.e. relative genetic variances). The total quantitative genetics pedigree design consisted of 8022 individuals (3981 females and 4041 males).

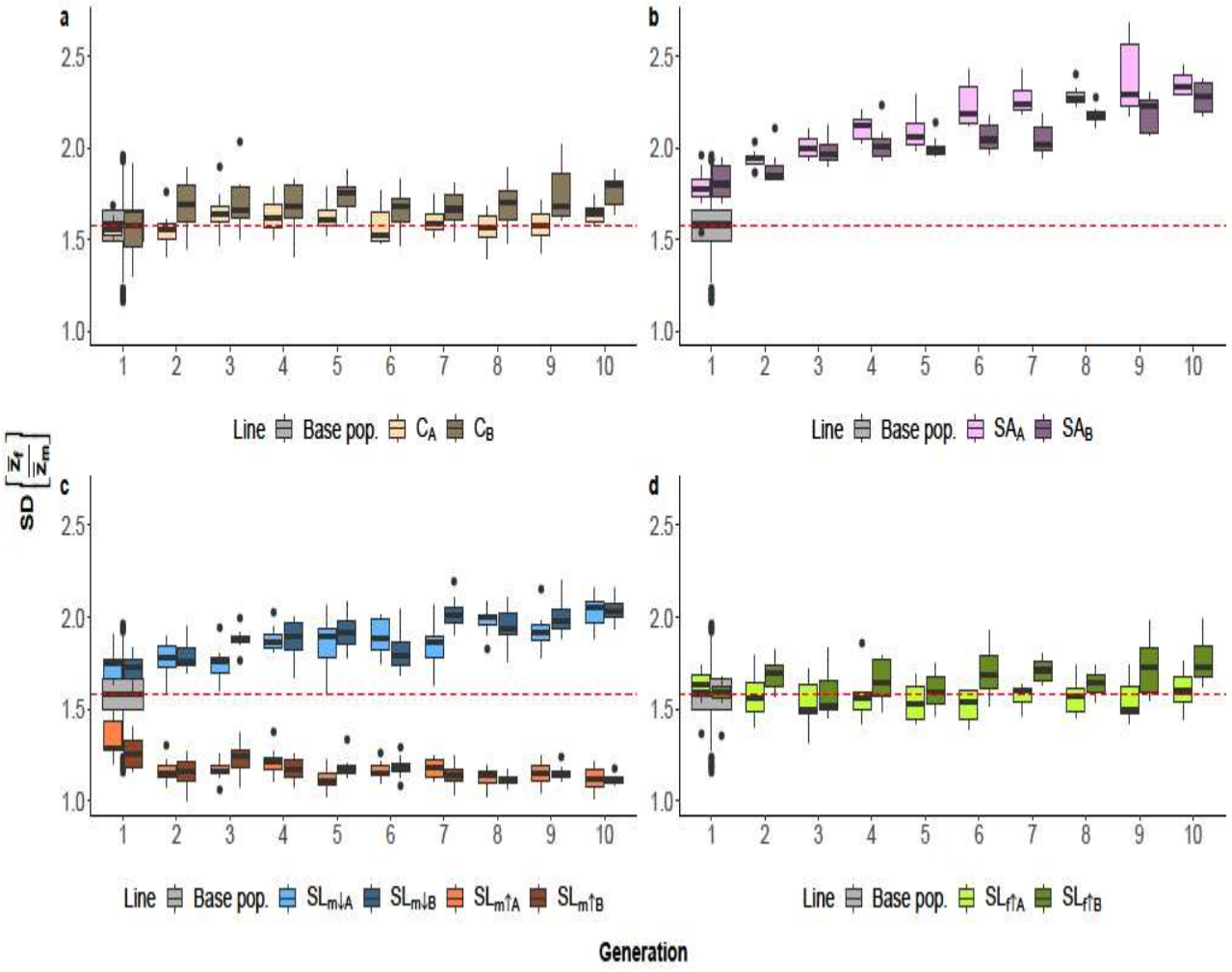

Fig. 2| Change in sexual dimorphism (SD) over the course of 10 generations of artificial family level selection. SD was measured as the ratio of the average female and average male body size. The boxplot in grey indicates the SD of the founding population for all lines (n = 161 families) and its average SD (red dashed line). Coloured boxplots depict the selected families (n = 8) in each line and generation under; **a)** random selection; **b)** sexually antagonistic selection; **c)** male limited selection (increased and decreased male body size in orange and blue, respectively); **d)** female limited selection for increased body size. In each family, SD was calculated as the ratio of the average female (n = 7) and male (n = 7) body size. Boxplots indicate the 25th, median and 75th percentiles, whiskers extend by 1.5 times the interquartile range.

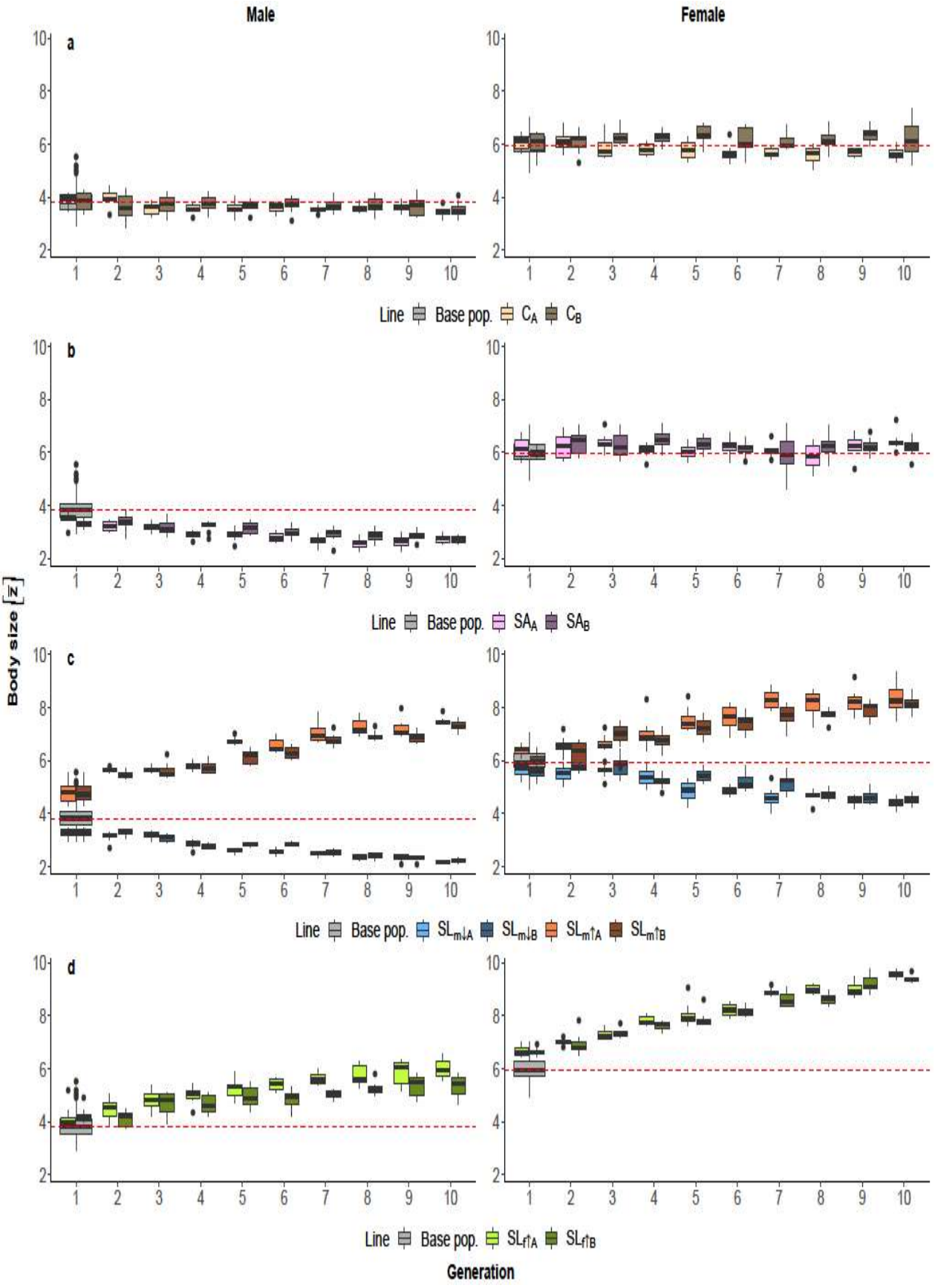

Fig. 3| **Trajectory of male (left) and female (right) body size evolution** under the five different selection regimes. Coloured boxplots depict the selected families (n = 8) in each replicate line and

generation under; **a)** random selection; **b)** sexually antagonistic selection; **c)** male limited selection (increased and decreased male body size in orange and blue, respectively); **d)** female limited selection for increased body size. The boxplots in grey depict the male (left) or female (right) body size of the ancestral population (G0) and the dashed, horizontal line shows the mean male and female body size at G0 as a reference. Boxplots indicate the 25^{th}, median and 75^{th} percentiles, whiskers extend by 1.5 times the interquartile range.

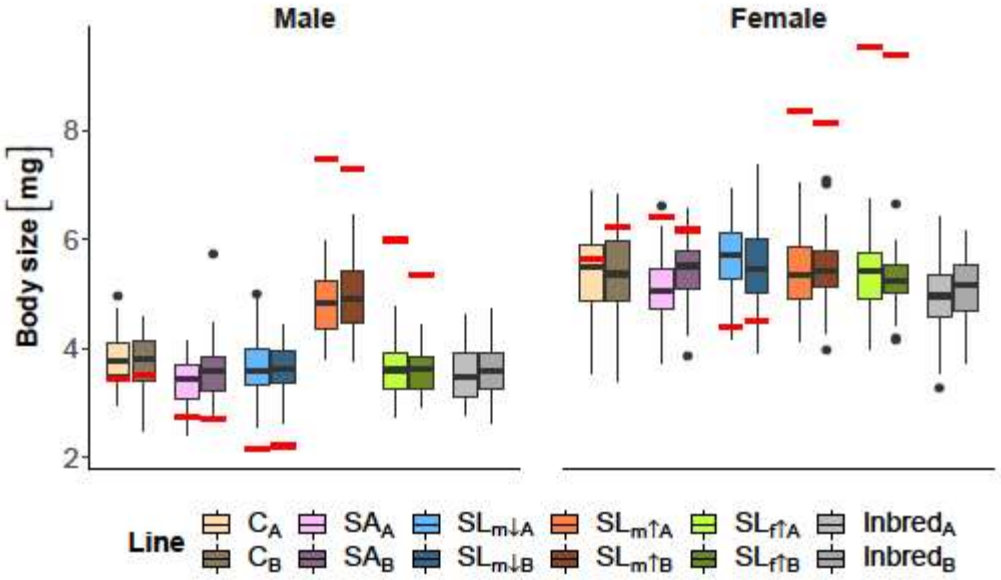

628

629 **Fig. 4| Effect of Y chromosome on body size after introgression into an isogenic background.**

630 Body size of males (n = 109) and females (n = 97) after 13-generations of introgression of the

631 selection lines to a common isogenic background (shown in grey, males n = 113; females n = 113).

632 The different colours represent the selection regime and replicate, the red bars indicate the average

633 body size directly after the artificial selection, before the introgression. After introgression the lines

634 became >99.97% identical to the background, apart from the non-recombining Y chromosome.

635 Introgression changed the sexual size dimorphism to the same level to that of the inbred background

636 in all other lines except those where males were selected for large size ($SL_m\uparrow$). In these lines the

637 males retained their significantly larger size, reducing the sex difference by 30%. Boxplots indicate

638 the 25th, median and 75th percentiles, whiskers extend by 1.5 times the interquartile range.

639

Extended Data Figures:

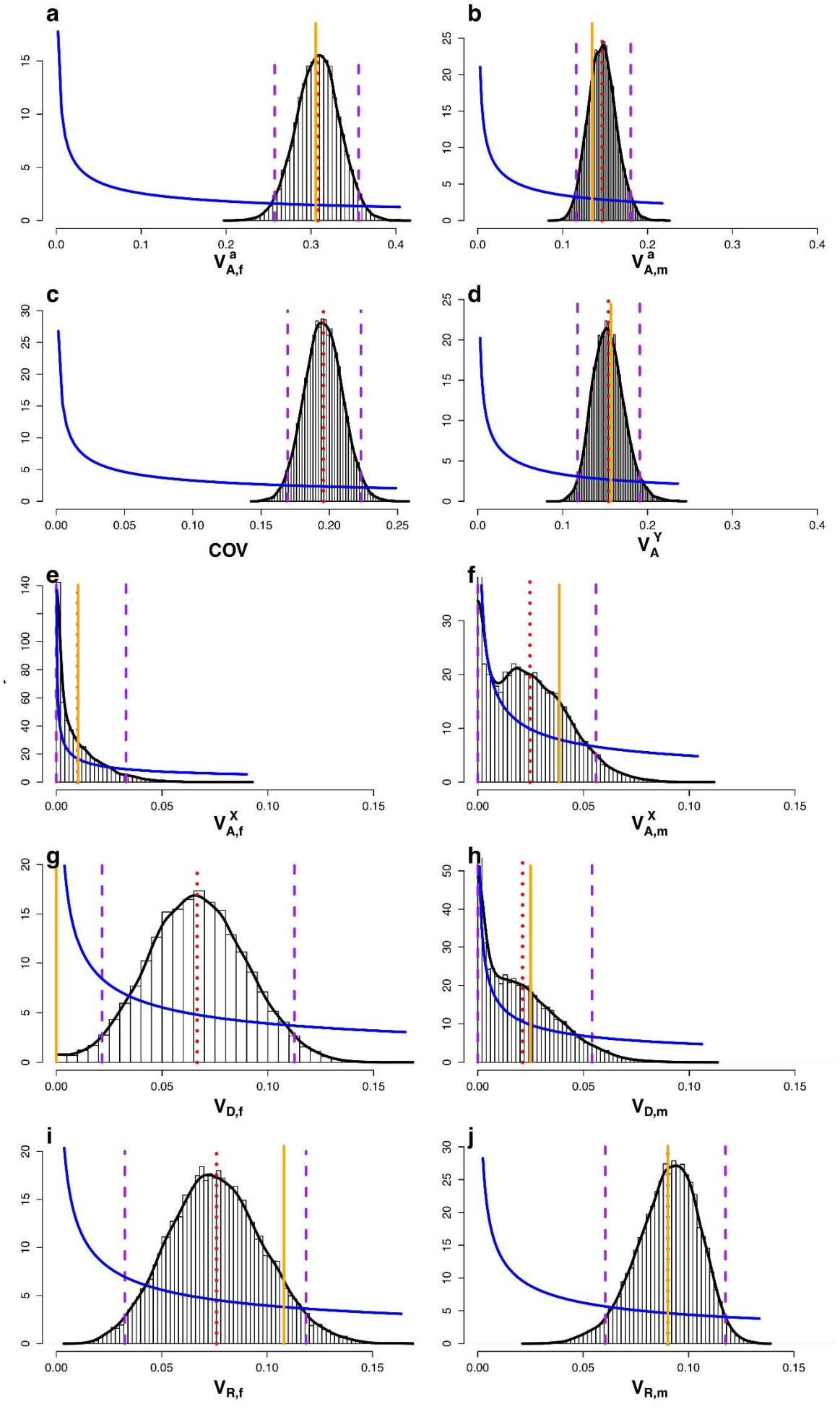

641

Extended Data Fig. 1| Genetic (co)variance estimates. Marginal posterior distribution of the genetic (co)variances in females and males as a histogram and density curve (black solid line), with the 95% credible intervals (purple dashed line), mean (red dotted line) and the prior distribution (blue solid line). Additionally, we also show the restricted likelihood based mean (yellow vertical line) for a comparison. a & b) Autosomal additive genetic variance is larger in females than in males. c) Genetic covariance between males and females d) Y-linked additive genetic variance. e & f) X-linked additive genetic variance in females and males. g & h) Dominance variance in females and males. i & j) Residual variance in females and males.

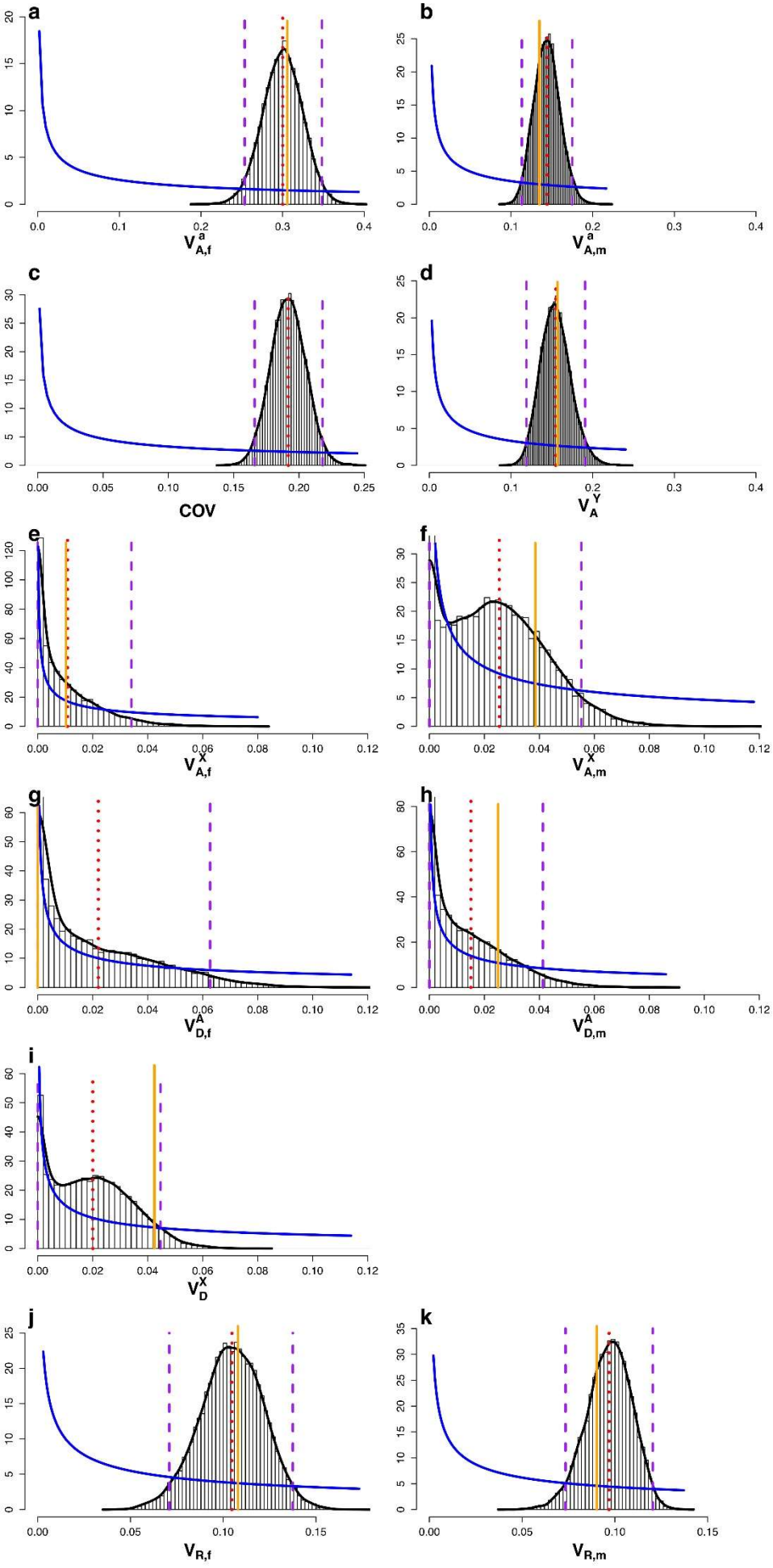
a
$V^{a}_{A,f}$
b
$V^{a}_{A,m}$
c
COV
d
V^{Y}_{A}
e
$V^{X}_{A,f}$
f
$V^{X}_{A,m}$
g
$V^{A}_{D,f}$
h
$V^{A}_{D,m}$
i
V^{X}_{D}
j
$V_{R,f}$
k
$V_{R,m}$

651

Extended Data Fig. 2| Genetic (co)variance estimates of a model with X-linked dominance variance partitioning. Marginal posterior distribution of the genetic (co)variances as a histogram and density (black solid line), 95% credible interval (purple dashed line), mean (red dotted line) and the prior distribution (blue solid line). Additionally, we also show the restricted likelihood based mean (yellow vertical line). a & b) Autosomal additive genetic variance is larger in females than in males. c) Genetic covariance between males and females. d) Y-linked additive genetic variance. e & f) X-linked additive genetic variance in females and males. g & h) Dominance variance in females and males. i) X-linked dominance variance in females. j & k) Residual variance in females and males.

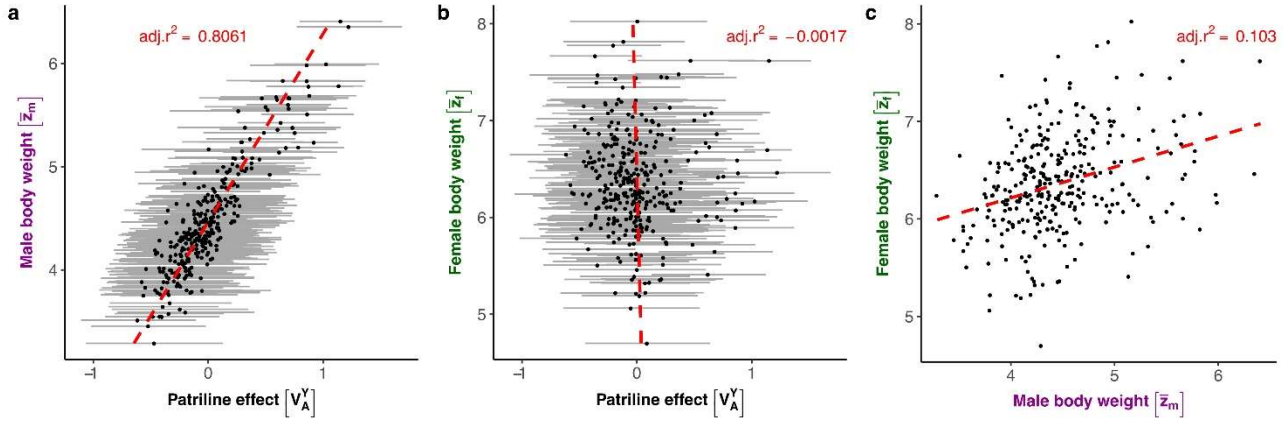

662

663 **Extended Data Fig. 3| Y-lineage effect in the pedigree analysis.** Estimated mean Y-lineage effect
664 and their 95% credible interval (grey bar) in the pedigree analysis. Positive values make males on
665 average larger while negative values make males on average smaller. a) There is a significant
666 positive correlation between Y-lineage effect and body size of males that carry this Y lineage (t
667 value = 16.61, p value = <0.0001). b) We see no correlation between the Y-lineage effect and the
668 body size of related females (t value = 0.014, p value = <0.989). c) Overall, there is a significant
669 positive correlation between male and female body size within patrilines.

670

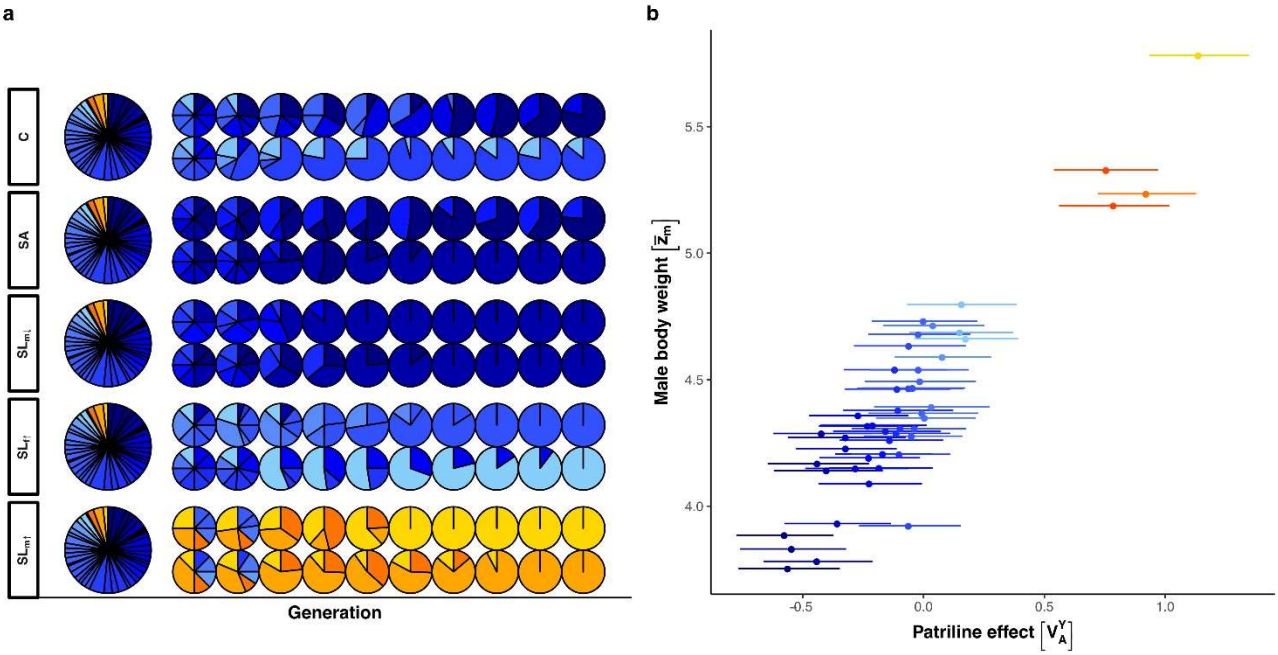

671

672 **Extended Data Fig. 4| Y-lineage frequency changes in response to artificial selection.** a) Y-
673 lineage frequency changes over the course of 10 generations of artificial selection in 5 different
674 selection regimes (C = drift control, SA = sexually antagonistic selection, SL = sex limited selection
675 for; m↓ small males, m↑ large males, f↑ large females), each selection regime has 2 replicate lines.
676 All selection lines started from the same ancestral population (G0), shown with the big circle. b)
677 The Y-lineages are colour coded according to their estimated effect on male body size. Note that Y-
678 lineage ≠ Y haplotype. The Y lineage represent each founder male (GGP) in our 4-generation
679 pedigree, and most of these Y lineages are likely the same haplotype (e.g. all Y lineages in dark
680 blue have a very similar effect on male body size).

681

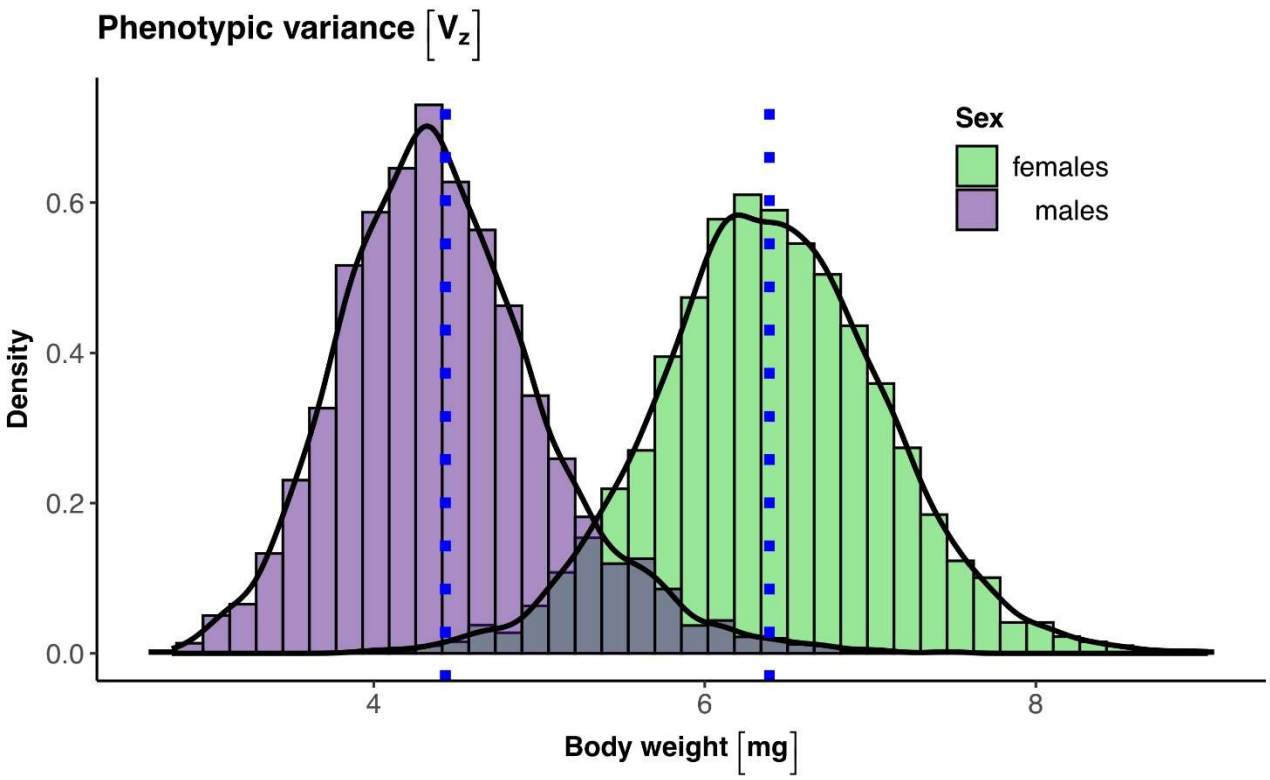

682

683 **Extended Data Fig. 5| Phenotypic body size variance in the pedigree population.** Body size is

684 normally distributed in both sexes, indicating that size is a polygenic trait. Males are on average

685 lighter than females ($\overline{z}_m$ = 4.43, $\overline{z}_f$ = 6.39) and body size is less variable in males than in females

686 ($\sigma^2_{z,m}$ = 0.410, $\sigma^2_{z,f}$ = 0.478, F = 0.857, df_{num} = 3702, df_{denum} = 3642, $p < 0.001$).

687

Rapid evolution of sexual size dimorphism facilitated by Y-linked genetic variance

Philipp Kaufmann, Matthew E. Wolak, Arild Husby, Elina Immonen

Supplementary Information

Supplementary Table 1: Posterior genetic variance estimates in a model that includes X-linked dominance: mean, [posterior mode] and (95% credible interval). Partitioning of the female dominance into autosomal and X-linked dominance suggests that a substantial part of the female dominance is due to X-linked dominance. The model was run on 16 independent Markov chains in parallel for 670,000 iterations (burnin 20,000, thinning interval 650) yielding 1,000 samples for each chain and 16,000 samples across all chains. Absolute autocorrelation values are < 0.16 and the effective sample size > 12,000 for each posterior distribution.

	Additive (co)variance					**Dominance variance**		**Maternal environment**	**Residual Variance**
	autosomal		X-linked	Y-linked	total	autosomal	X-linked		
Female body size	$\mathbf{V^a_{A,f}}$ **= 0.300** [0.301] (0.254,0.348)	$\mathbf{COV^a_A}$ **= 0.192** [0.193] (0.166,0.218)	$V^X_{A,f}$ = 0.011 [0.000] (0.000,0.034)		$\mathbf{V_{A,f}}$ **= 0.311** [0.305] (0.267,0.353)	$V^a_{D,f}$ = 0.022 [0.000] (0.000,0.063)	$V^X_{D,f}$ = 0.020 [0.000] (0.000,0.045)	$V_{ME,f}$ = 0.004 [0.000] (0.000,0.012)	$\mathbf{V_{R,f}}$ **= 0.105** [0.107] (0.071,0.138)
Male body size	$\mathbf{V^a_{A,m}}$ **= 0.144** [0.142] (0.113,0.175)	$\mathbf{r^a_{m,f}}$ **= 0.925** [0.928] (0.847,0.994)	$V^X_{A,m}$ = 0.025 [0.000] (0.000,0.055)	$\mathbf{V^Y_A}$ **= 0.155** [0.155] (0.119,0.191)	$\mathbf{V_{A,m}}$ **= 0.324** [0.317] (0.274,0.378)	$V_{D,m}$ = 0.015 [0.000] (0.000,0.041)		$V_{ME,m}$ = 0.002 [0.000] (0.000,0.007)	$\mathbf{V_{R,m}}$ **= 0.097** [0.101] (0.073,0.120)
Sexual dimorphism	$\mathbf{V^a_{SSD}}$**= 0.061** [0.055] (0.026,0.100)								
Female heritability	$\mathbf{h^2_{a,,f}}$ **= 0.679** [0.671] (0.583,0.772)		$h^2_{X,f}$ = 0.024 [0.000] (0.000,0.076)		$\mathbf{h^2_{t,A,f}}$ **= 0.704** [0.709] (0.627,0.782)				
Male heritability	$\mathbf{h^2_{a,,m}}$ **= 0.329** [0.321] (0.258,0.404)		$h^2_{X,m}$ = 0.057 [0.001] (0.000,0.122)	$\mathbf{h^2_{Y,m}}$ **= 0.352** [0.356] (0.296,0.411)	$\mathbf{h^2_{t,A,m}}$ **= 0.739** [0.743] (0.675,0.797)				

Supplementary Table 2: Posterior genetic variance estimates mean, [posterior mode] and (95% credible interval) in a model that did not include Y-linked variance (i.e. restricted V_A^Y to be zero). Estimates that changed significantly (i.e. are outside of the 95% credible interval of the more complex model that includes V_A^Y partition, as presented in the main text) are highlighted with ‡ or ⸸ if they are significantly overestimated or underestimated, respectively. Values in bold are significantly different from zero. Both models were run on 16 independent Markov chains in parallel for 670,000 iterations (burnin 20,000, thinning interval 650) yielding 1,000 samples for each chain and 16,000 samples across all chains. Absolute autocorrelation values are < 0.125 and the effective sample size > 11,500 for each posterior distribution.

	Additive (co)variance					**Dominance variance**	**Maternal environment**	**Residual Variance**
	autosomal		X-linked	Y-linked	total			
Female body size	$\mathbf{V_{A,f}^a = 0.292}$ [0.299] (0.229,0.356)	$\mathbf{COV_A^a = 0.180}$ [0.173] (0.149,0.209)	$V_{A,f}^X = 0.029$ [0.000] (0.000,0.070)		$\mathbf{V_{A,f} = 0.322}$ [0.321] (0.277,0.369)	$\mathbf{V_{D,f}^a = 0.061}$ [0.068] (0.009,0.106)	$V_{ME,f} = 0.005$ [0.000] (0.000,0.017)	$\mathbf{V_{R,f} = 0.082}$ [0.080] (0.036,0.131)
Male body size	$\mathbf{V_{A,m}^a = 0.287}$ ‡ [0.287] (0.250,0.320)	$\mathbf{r_{m,f}^a = 0.624}$ ⸸ [0.633] (0.514,0.727)	$\mathbf{V_{A,m}^X = 0.061}$ [0.047] (0.009,0.110)	$V_A^Y = 0.000$ [0.000] (0.000,0.000)	$\mathbf{V_{A,m} = 0.347}$ [0.336] (0.287,0,418)	$V_{D,m} = 0.033$ [0.033] (0.000,0.064)	$V_{ME,m} = 0.003$ [0.000] (0.000,0.008)	$\mathbf{V_{R,m} = 0.020}$ ⸸ [0.017] (0.005,0.034)
Sexual dimorphism	$\mathbf{V_{SSD}^a = 0.219}$ ‡ [0.209] (0.143,0.294)							
Female heritability	$\mathbf{h_{a,,f}^2 = 0.623}$ [0.645] (0.502,0.742)		$h_{X,f}^2 = 0.062$ [0.001] (0.000,0.149)		$\mathbf{h_{t,A,f}^2 = 0.685}$ [0.687] (0.613,0.756)			
Male heritability	$\mathbf{h_{a,,m}^2 = 0.713}$ ‡ [0.696] (0.637,0.787)		$\mathbf{h_{X,m}^2 = 0.148}$ [0.187] (0.028,0.258)	$h_{Y,m}^2 = 0.000$ ⸸ [0.000] (0.000,0.000)	$\mathbf{h_{t,A,m}^2 = 0.861}$ [0.882] (0.776,0.948)			

Supplementary Table 3: Type III sum of squares ANOVA table for the evolution of SD over the course of 10 generations of the artificial selection in 5 different selection regimes, with two replication lines in each selection regime. Mixed effect model: SD~Regime*Generation + (1 | Line).

	χ^2	*df*	*p-value*
Intercept	1521.25	1	<0.001***
Generation	5.04	1	0.0248*
Regime	107.64	4	<0.001***
Generation x Regime	317.78	4	<0.001***

Supplementary table 4: ASREML likelihood ratio model comparisons. Model **A:** the full model, using the same fixed and random effects as described for the Bayesian model in the main text (see ASReml R code). Model **B:** female and male dominance variance restricted to be equal. Model **C:** female and male additive X linked genetic variance restricted to be equal. Model **D:** female additive X linked genetic variance restricted to be zero. Model **E:** male additive X-linked genetic variance restricted to be zero.

Model comparison	LRT_{df}	*p-value*
A vs. B $(\boldsymbol{V_{D,f} = V_{D,m}})$	$\chi^2_{1:0} = 3.433$	$\mathbf{0.032}$
A vs. C $(\boldsymbol{V^X_{A,f} = V^X_{A,m}})$	$\chi^2_{1:0} = 0.869$	0.176
A vs. D $(\boldsymbol{V^X_{A,m} = 0})$	$\chi^2_{1:0} = 3.472$	$\mathbf{0.031}$
A vs. E $(\boldsymbol{V^X_{A,f} = 0})$	$\chi^2_{1:0} = 0.351$	0.277

Model comparison suggests significantly higher dominance variance for body size in females than in males, i.e., the data fits a model with sex-specific dominance variance significantly better compared to a model where we restrict the dominance to be equal in the sexes (A vs. B). While the model comparisons further suggest a significant X-linked additive genetic variance (V_A^X) in males (A vs. D) but not in females (A vs. E), a direct comparison between $V_{A,f}^X$ and $V_{A,m}^X$ (A vs. C) shows no significant difference.

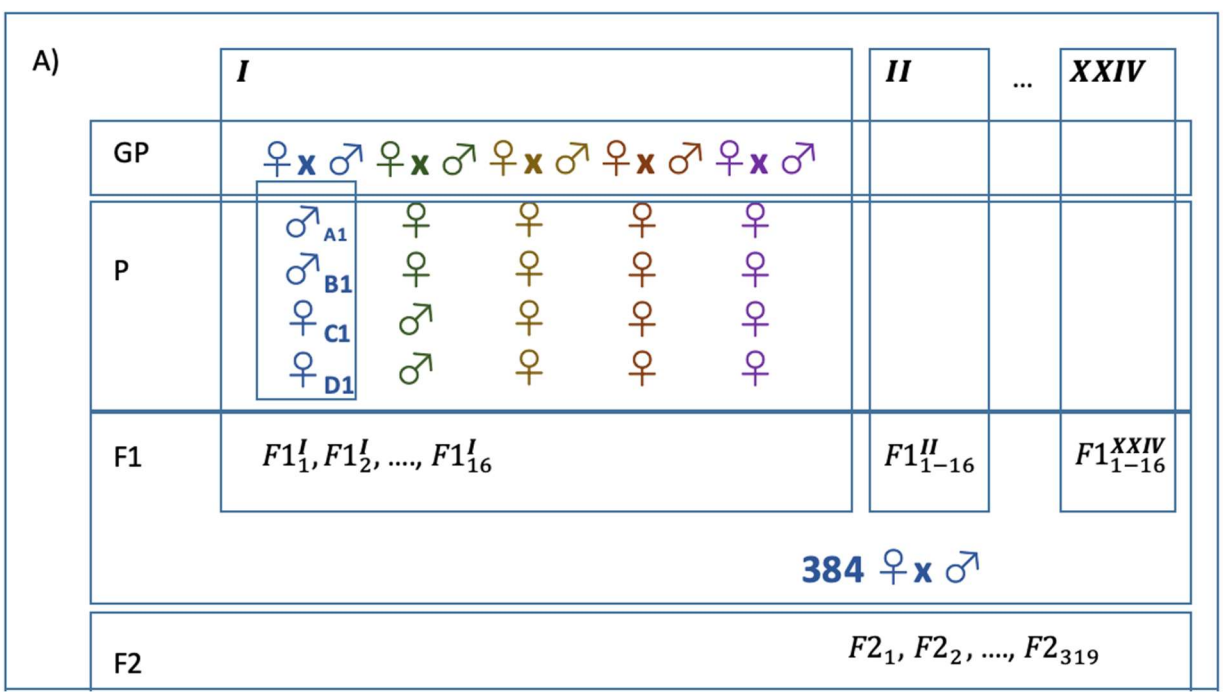

718

719 **Additional Supplementary Figure 1: Overview breeding design:** In each breeding set we
720 randomly paired 10 unrelated GP, yielding 5 parental families (P1-P5). P males from family P1 &
721 P2 were paired consecutively with females of the 4 different parental families, respectively,
722 yielding 16 paternal half-sib F1-families. The breeding set was replicated 24 times (384 F1-families
723 in total). The F2 generation was created by randomly pairing F1 individuals from across all 24
724 replicates, each F1-family contributed 1 male and 1 female, respectively, yielding 311 F2 families.
725 The total breeding design consists of 8022 individuals.

726

Animal model as presented in the main text

MCMCglmm

```
############ prior ############
prior6.0 <- list(R=list(R1=list(V=diag(c(varF,varM)), nu=(1)/4)),#units
                 G=list(G1=list(V=diag(2), nu=2+1, alpha.mu=rep(0, 2), alpha.V=diag(2)*1000),#VAa
                        G2=list(V=diag(2), nu=2+1, alpha.mu=rep(0, 2), alpha.V=diag(2)*1000),#VAx
                        G3=list(V=diag(2), nu=2+1, alpha.mu=rep(0, 2), alpha.V=diag(2)*1000),#VD
                        G4=list(V=diag(2), nu=2+1, alpha.mu=rep(0, 2), alpha.V=diag(2)*1000),#VME
                        G5=list(V=diag(1), nu=1+1, alpha.mu=rep(0, 1), alpha.V=diag(1)*1000)))#VAy

############ model ############
Nrc <- nrow(phenADSb)
cores <- 16

model_6.0 <- mclapply(1:cores, function(i){
  set.seed(111+i)

####### Starting values
  StartN <- list(liab = rnorm(n = Nrc, mean = 0, sd = 12),
        R = list(R1 = rIW(V = diag(2), nu = 15)),
        G = list(G1 = rIW(V = diag(2), nu = 15),
                 G2 = rIW(V = diag(2), nu = 15),
                 G3 = rIW(V = diag(2), nu = 15),
                 G4 = rIW(V = diag(2), nu = 15),
                 G5 = rIW(V = diag(1), nu = 15)))


########## MCMC
  MCMCglmm(BODYSIZE~SEX*SEQ + poly(TIME,2,raw = TRUE) +SEX:poly(TIME,2,raw = TRUE),
           random = ~us(SEX):animal + idh(SEX):animalS + idh(SEX):animalD
           + idh(SEX):CYTO_n + Y_n,
           rcov = ~idh(SEX):units,
           start = StartN,
           ginverse = list(animal=Ainv, animalS=Sinv, animalD=Dinv),
           prior = prior6.0,
           data = phenADSb, family = 'gaussian'
           , nitt = 670000, thin =650, burnin = 20000,
           saveZ = TRUE, saveX = TRUE, saveXL = TRUE, pr = TRUE
           )
}, mc.cores = cores)
```

ASReml-R 4.0

```
asreml::asreml(WEIGHT~SEX+SEQ+SEX:SEQ+DEV.TIME+SEX:DEV.TIME+Line+Line:SEX,
                      random = ~corgh(SEX):vm(animal,AINV)
                      + ~idh(SEX):vm(animalD,Dinv)
                      + ~idh(SEX):vm(animalS,Sinv)
                      + ~at(SEX, 'M'):Y
                      + ~idh(SEX):Me,
                      residual =  ~dsum(~idv(units)|SEX),
                      data = NQG.data,
                      workspace = "8gb",
                      maxit = 50)
```

Animal model with X-linked dominance variance partitioning

MCMCglmm

```
############ prior ############
prior6.0 <- list(R=list(R1=list(V=diag(c(varF,varM)), nu=2)),#units
                 G=list(G1=list(V=diag(2)*0.02, nu=2+1, alpha.mu=rep(0, 2), alpha.V=diag(2)*1000),#VAa
                        G2=list(V=diag(2)*0.02, nu=2+1, alpha.mu=rep(0, 2), alpha.V=diag(2)*1000),#VAx
                        G3=list(V=diag(2)*0.02, nu=2+1, alpha.mu=rep(0, 2), alpha.V=diag(2)*1000),#VD
                        G4=list(V=diag(2)*0.02, nu=2+1, alpha.mu=rep(0, 2), alpha.V=diag(2)*1000),#VME
                        G5=list(V=diag(1)*0.02, nu=1+1, alpha.mu=rep(0, 1), alpha.V=diag(1)*1000),#VAy
                        G6=list(V=diag(1)*0.02, nu=1+1, alpha.mu=rep(0, 1), alpha.V=diag(1)*1000)))#VDx

############ model ############
Nrc <- nrow(phenADSb)
cores <- 16

model_6.0 <- mclapply(1:cores, function(i){
  set.seed(111+i)

####### Starting values
# creating list with starting values
  StartN <- list(liab = rnorm(n = Nrc, mean = 0, sd = 12),
        R = list(R1 = rIW(V = diag(2), nu = 15)),
        G = list(G1 = rIW(V = diag(2), nu = 15),
                 G2 = rIW(V = diag(2), nu = 15),
                 G3 = rIW(V = diag(2), nu = 15),
                 G4 = rIW(V = diag(2), nu = 15),
                 G5 = rIW(V = diag(1), nu = 15),
                 G6 = rIW(V = diag(1), nu = 15)))


########## MCMC
  MCMCglmm(BODYSIZE~SEX*SEQ + poly(TIME,2,raw = TRUE) +SEX:poly(TIME,2,raw = TRUE),
           random = ~us(SEX):animal + idh(SEX):animalS + idh(SEX):animalD
           + idh(SEX):CYTO_n + Y_n+ animalSd,
           rcov = ~idh(SEX):units,
           start = StartN,
           ginverse = list(animal=Ainv, animalS=Sinv, animalD=Dinv, animalSd=Sdinv),
           prior = prior6.0,
           data = phenADSb, family = 'gaussian'
           , nitt = 670000, thin =650, burnin = 20000,
        saveZ = TRUE, saveX = TRUE, saveXL = TRUE, pr = TRUE
           )
}, mc.cores = cores)
```

ASReml-R 4.0

```
asreml::asreml(WEIGHT~SEX+SEQ+SEX:SEQ+DEV.TIME+SEX:DEV.TIME+Line+Line:SEX,
                      random = ~corgh(SEX):vm(animal,AINV)
                      + ~idh(SEX):vm(animalD,Dinv)
                      + ~idh(SEX):vm(animalS,Sinv)
                      + ~at(SEX, 'F'):vm(animalSd,Sdinv)
                      + ~at(SEX, 'M'):Y
                      + ~idh(SEX):Me,
                      residual =  ~dsum(~idv(units)|SEX),
                      data = NQG.data,
                      workspace = "8gb",
                      maxit = 50)
```

Animal model without Y-linked additive variance partitioning

MCMCglmm

```
############ prior ############
prior6.0 <- list(R=list(R1=list(V=diag(c(varF,varM)), nu=1/4)),#units
                 G=list(G1=list(V=diag(2), nu=2+1, alpha.mu=rep(0, 2), alpha.V=diag(2)*1000),#VAa
                        G2=list(V=diag(2), nu=2+1, alpha.mu=rep(0, 2), alpha.V=diag(2)*1000),#VAx
                        G3=list(V=diag(2), nu=2+1, alpha.mu=rep(0, 2), alpha.V=diag(2)*1000),#VD
                        G4=list(V=diag(2), nu=2+1, alpha.mu=rep(0, 2), alpha.V=diag(2)*1000)))#VME



############ model ############
Nrc <- nrow(phenADSb)
cores <- 16

model_6.0_wo_Y <- mclapply(1:cores, function(i){
  set.seed(111+i)

####### Starting values
  StartN <- list(liab = rnorm(n = Nrc, mean = 0, sd = 12),
        R = list(R1 = rIW(V = diag(2), nu = 15)),
        G = list(G1 = rIW(V = diag(2), nu = 15),
                 G2 = rIW(V = diag(2), nu = 15),
                 G3 = rIW(V = diag(2), nu = 15),
                 G4 = rIW(V = diag(2), nu = 15)))


########## MCMC
  MCMCglmm(BODYSIZE~SEX*SEQ + poly(TIME,2,raw = TRUE)+SEX:poly(TIME,2,raw = TRUE),
           random = ~us(SEX):animal + idh(SEX):animalS + idh(SEX):animalD
           + idh(SEX):CYTO_n,
           rcov = ~idh(SEX):units,
           start = StartN,
           ginverse = list(animal=Ainv, animalS=Sinv, animalD=Dinv),
           prior = prior6.0,
           data = phenADSb, family = 'gaussian'
           , nitt = 670000, thin = 650, burnin = 20000
           )
}, mc.cores = cores)
```